

# Design, construction and characterization of a diagnostic for measuring the pulse contrast in a high intensity laser

Ana Castanheira

*Institute for Plasmas and Nuclear Fusion, Instituto Superior Tecnico, Lisbon, Portugal*

November 24, 2011

## Abstract

We describe the design, construction and implementation of a high dynamic range, third-order contrast-ratio measurement diagnostic for a high power laser chain. The device, known as Optical Parametric Amplification Correlator (OPAC) is based on degenerate three-wave mixing in a nonlinear crystal, it is self-referencing and compact. By measuring the idler pulse with a slow detector and a set of calibrated filters, a dynamic range of up to  $10^{10}$  is achievable. The pulse contrast is to be characterized at the mJ-level, 10 Hz, Ti:sapphire pre-amplifier stage, in a time window of 100 ps

**Keywords:** Pulse characterization, high power pulses, temporal contrast, optical parametric amplification

## 1 Introduction

High power lasers have experienced a tremendous evolution over the last two decades [1], with a systematic increase in the focused intensity and a decrease in the pulse duration leading to current state-of-the-art petawatt-level systems capable of delivering focused intensities in excess of  $10^{22}$  W/cm<sup>2</sup> [2]. Such tremendous intensities find applications in many fields, such as high-order harmonic generation, x-ray sources, particle acceleration and ultra-relativistic laser matter interaction, especially when the pulse duration is of the order of only a few optical cycles (<20 fs).

A critical issue for all ultrahigh intensity laser systems is the achievable temporal contrast, i.e. the ratio between the intensity of the main pulse and that of any feature around it, in a time window typically extending into the ns range. These include any pre- or post-pulses, caused e.g. by spurious reflections or low-contrast polarization optics in multipass or regenerative amplifiers, and the long pedestal associated to amplified spontaneous emission arising from the decay of inverted population in traditional laser amplification. In particular, pre-pulses can be highly detrimental for experi-

ments involving interaction with a solid target, leading to the formation of a pre-plasma before the arrival of the main, high intensity pulse, and modifying the expected interaction regime. For state-of-the-art lasers, the contrast requirement can be as high as  $10^{11}$ , which poses considerable challenges both for its generation and its characterization [3].

Concerning the generation of ultrahigh contrast pulses, a number of advanced techniques are currently employed, resorting to temporal filtering at either the high or low energy levels. An example of the former consists in implementing plasma mirrors after the compressor in a typical chirped pulse amplification setup [4] which provides limited success at the cost of a significant fraction ( $\sim 50\%$ ) of the energy. Nonlinear, low energy level filtering has been demonstrated e.g. through the cross-polarized wave technique [5], which allows efficient cleaning of ASE, and has shown to be scalable to petawatt, sub-15 fs pulses with a predicted contrast of up to  $10^{12}$ .

Characterizing high power laser pulses over such a wide dynamic range is a problem far from being trivial. The diagnostic must be sensitive enough over more than 10 orders of magnitude, reliable, and capable of

measuring over a time window that can extend up into the hundreds of ps. All devices for characterizing the temporal behavior of ultrashort pulses are based on nonlinear correlation techniques, typically involving correlation of the pulse with itself, or autocorrelation. There is a fundamental reason for this, which is that in order to characterize a short event, an event of shorter duration is required; in its absence, the only solution is to use the event itself as a time gate. Nonlinear combination in a birefringent crystal has proved a simple and popular technique for providing the optical equivalent of the mathematical autocorrelation function, thus allowing an estimate of the original pulse duration, provided we make an assumption about the temporal pulse profile. Second order autocorrelation is capable of measuring pulse contrasts up to  $10^8$  at the low power, oscillator level [6, 7]. However, this technique is unable to distinguish between pre- and post-pulses, which appear symmetrically placed around the main pulse, posing a serious limitation in view of the remarks above. To overcome this undesirable characteristic we can use a third order correlator that time-gates the pulse with a frequency-doubled version of itself, by mixing them in a third order nonlinear crystal, and measuring the resulting third harmonic signal [8, 9]. Eventual pre- and post-pulses will still appear located symmetrically around the main pulse, but it is possible to distinguish them because now they will have different magnitudes depending on their origin. When we have a repetitively pulsed laser with a comfortable ( $\sim$ Hz-MHz) repetition rate, this method can be used to build the autocorrelation trace by scanning the relative time delay between the test and the probe pulses. For low repetition rate ( $<$ Hz) laser systems, single shot versions have also been demonstrated [10]-[12]. Third order autocorrelation is indeed a powerful technique that has attracted much attention over the years, and capability of measuring contrast ratios of up to  $10^{10}$  has been demonstrated [13].

The main limitations of this approach are the low efficiency associated to the third-order generation process, the noise level of the detector, and the fact that the third harmonic of typical high power laser systems operating in the near infrared lies in the ultraviolet wavelength region. An effective approach for dealing with all these issues consists in amplifying the original signal, i.e. using the gating pulse to amplify selectively a narrow time window of the test pulse. This has the additional advantage of increasing the signal-to-noise ratio of the

detector and thus also the dynamic range of the diagnostic. To achieve this we can replace the third-order process by an optical parametric amplifier (Figure 1), an approach similar to a technique already used to measure the amplitude and phase of weak, short pulses [14, 15]. In this case, we speak of an optical parametric amplifier correlator (OPAC) [16]. In this degenerate configuration the pump beam, at twice the original frequency, is used to amplify the seed beam, generating a third (idler) beam at the same fundamental frequency. The idler beam appears due to energy and momentum conservation requirements, and indeed is only present when both the pump and the seed beam (or any signal in this beam) overlap in the nonlinear crystal. A noncollinear geometry (i.e. introducing a small angle between the two beams) is required in order to separate spatially the idler and the signal beams.

This technique exhibits two important advantages: reduction of the background noise because the measured signal is spatially shifted, and signal amplification (up to  $10^6$  is a common figure for an OPA), so the measurement is no longer limited by the detector noise. However, since the OPAC is used at degeneracy, one has to be careful with the scattered signal light, because this could limit the overall performance. To minimize the scattered light we can e.g. increase the non-collinear angle and use adequate spatial filtering.

In this work, we present the design and implementation study for an OPAC, with the purpose of characterizing a 20 TW laser chain operating at 1053 nm. The proposed OPAC is fully computer controlled, occupies a compact footprint, and is composed of readily available optical components.

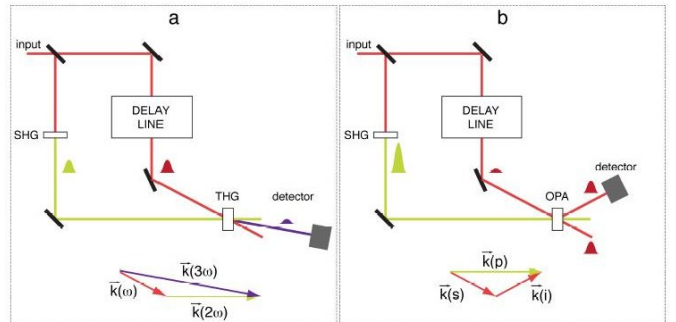


Figure 1: Schematic of (a) third-order autocorrelator and (b) optical parametric amplifier correlator. SHG/THG: second/third harmonic generation crystals, OPA: optical parametric amplification crystal. Also shown are the corresponding wavevector geometries, in the first case involving the fundamental, 2<sup>nd</sup> and 3<sup>rd</sup>

harmonic beams, and in the second involving the pump (p), seed (s) and idler (i) beams.

## 2 Experimental Implementation

The laser to be characterized is the multi-terawatt, hybrid Ti:sapphire-Nd:glass, chirped pulse amplification system at the Laboratory for Intense Lasers (IST, Lisbon)[17]. The front end of this laser starts with a Ti:sapphire Kerr-lens modelocked oscillator (Mira 900F, Coherent Inc.) that delivers a  $\sim 120$  fs, 76 MHz pulse train with an average energy of 4 nJ per pulse at a central wavelength 1053 nm. These pulses are then stretched to  $\sim 900$  ps in an Öffner type grating stretcher and directed into a homemade, Nd:YAG pumped, linear Ti:sapphire regenerative amplifier operating at 10 Hz. Here their energy is raised up to  $\sim 2$  mJ, with an output spectral bandwidth of  $\sim 5$  nm. The high energy amplification section consists of two double-passed Nd:phosphate amplifiers in series (Quantel), with 16 and 45 mm diameters. The maximum obtainable energy, limited by B-integral, is up to 10 J, in 4 shots/hour. Finally, the pulses are compressed in a vacuum enclosed grating compressor, leading to a final pulse duration of  $\sim 400$  fs. Given the low repetition rate of the full laser, and the scanning nature of the OPAC, for this diagnostic the characterization will be performed at the front-end output (2 mJ, 10 Hz, 280 fs), using a secondary grating compressor. In general, any pre-pulses will arise during this stage, typically due to the output contrast of the regenerative amplifier, so the limitation is not critical.

In figure 2 is possible to observe the experimental layout. The compressed 2 mJ, 280 fs pulses are image relayed towards the OPAC and demagnified from 11 to 3 mm by using a telescope. This input beam is split into two by using a polarization-tunable 90/10 beam sampler, with most of the energy going in to the (transmitted) “pump” arm. The pump beam is generated by frequency doubling in a 1 mm thick BBO (beta-barium borate) crystal, where the input image plane of the OPAC is relayed. A dichroic mirror allows separating the green (526 nm) pulse from any remaining fundamental radiation, also serving to check the alignment of the input beam. An additional infrared filter is used to further clean the pump pulse. Meanwhile, the signal beam is sent on a variable length delay line, in order to match the optical path of the pump beam arm. Rough adjustment of the length is provided by a manually op-

erated translation stage, fine adjustment by an electronically controlled motorized translation stage (Newport MM3000 and MFN 25). A calibrated set of several neutral density filters allows attenuation of the transmitted energy up to  $10^6$ . This beam is also demagnified and image relayed to the BBO nonlinear crystal where interaction takes place. Here, the two beams overlap at a small angle, such that the idler beam is generated at a symmetrical angle relative to the pump beam. The idler beam is isolated by means of an iris, for minimizing noise, sent through a low-pass filter and finally detected by a large area amplified photodetector (PDA36A-EC, Thorlabs), with a gain adjustment range of 70 dB.

One of the main requirements for this setup was the need for a transportable, compact footprint, due to restrictions in the available laboratory space at the measurement location. With this in mind, the whole setup was fitted in a 60 by 30 cm aluminum breadboard, allowing easy integration and removal

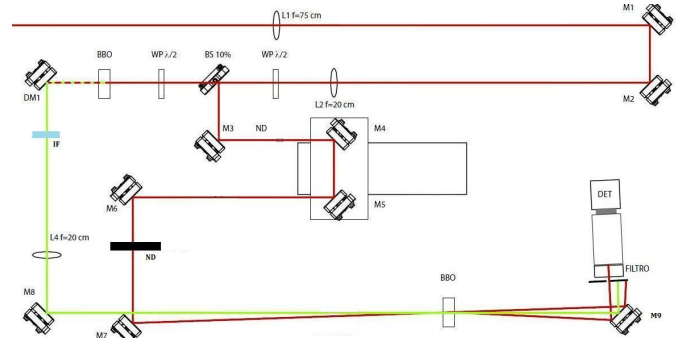


Figure 2: Layout of OPAC. L1-L4: lenses, M1-M8: mirrors, WP: waveplates, BBO: BBO nonlinear crystal, DM: dichroic mirror, ND: set of calibrated neutral density filters, DET: photodiode detector, IF: infra-red filter.

The photodiode output is connected to an oscilloscope (Tektronix DPO3014, 100 MHz, 2.5 GS/second). The controller for the translation stage is also connected to the same computer. A LabVIEW code was written, adapting the existing drivers, and allowing the user to adjust the measurement range and parameters, such as the number of averaging shots per position and the delay steps. The code allows the OPAC to run independently over a full measurement cycle, thanks to the computer automatically recording the idler intensity at each point, perform a given user-defined number of acquisitions, and translating the motorized stage to the next position, thereby building the full autocorrelation trace. This capability is essential for a long time window: for instance, at a 25 fs resolution (the narrowest allowed

by the translation stage resolution), and considering a time window of 100 ps, the acquisition will take 120 min. For the calculation of these values we took into consideration the fact that the laser operates a 10 Hz. Once the main features appearing in the trace are located, one can repeat the measurement and (manually) change the signal beam attenuation, while keeping the signal from the photodetector from reaching saturation, or increase the number of averaging shots for improved accuracy. The measurement is concluded once a non-saturated trace is obtained for the whole time window, and the traces for each attenuation are concatenated into a single one ([16]).

### 3 Experimental results

After assembling the OPAC we captured the beam profile for the several beams involved, before and after the OPA crystal. The results for the signal and idler after the crystal can be seen in figure 3, showing that both beams have a soft and regular spatial profile.

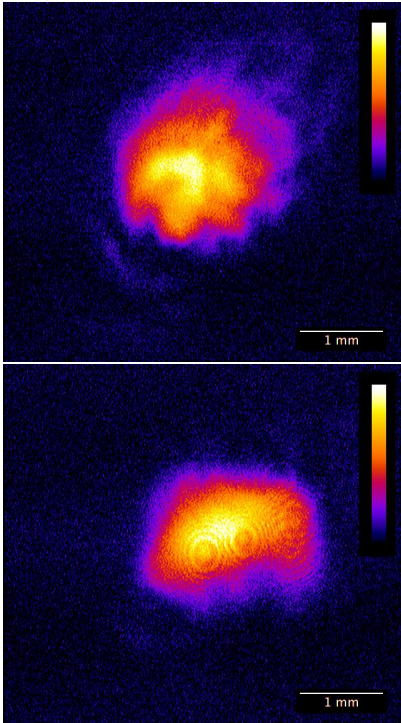


Figure 3: Signal (top) and idler (bottom) beams after the OPA crystal.

#### 3.1 OPAC as a 3<sup>rd</sup>-order autocorrelator

We first operated the OPAC as a regular third-order autocorrelator, over the range -1 to 1 ps around the main

pulse. Figure 4 shows the measured data, adjusted to a Gaussian curve. The resulting FWHM pulse duration is 220 fs. This value is compatible with previous measurements with other methods like second order autocorrelation, SPIDER and SHG FROG. This allows us to confirm that the OPAC is performing correctly.

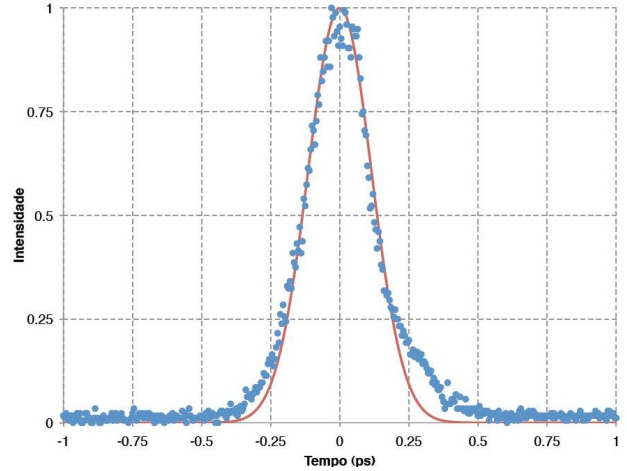


Figure 4: Measured third-order autocorrelation (blue dots) and Gaussian fit (red line).

#### 3.2 Contrast measurement over long time window

Next we operated the OPAC over a long time window extending from -50 to 50 ps, without attenuating the signal. This allowed us to register several low-amplitude satellite pulses, but also to detect some imperfections in the current setup, mostly due to mechanical components and sensitivity to alignment (see Figure 5).

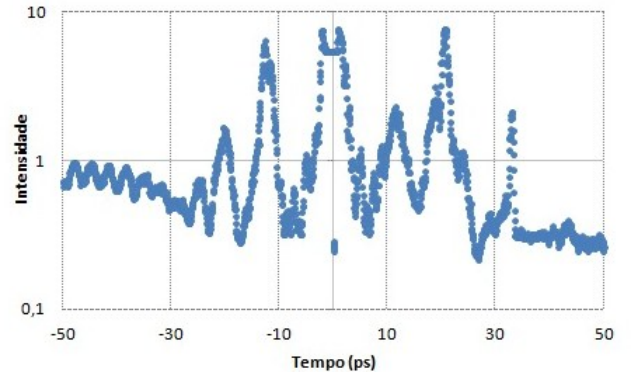


Figure 5: OPAC measurement over a 100 ps window.

Between -60 ps and -30 ps, we may notice two artifacts: a bump between 0.4 and 1.0, and an oscillation with a period of  $\sim 5$  ps. We believe that the first is related to an imperfect alignment of the delay line, and the second is caused by a mechanical defect in the trans-

lation of the motor during the scan. It is also possible see a plateau in the main pulse (-2 to 2 ps) due to the saturation of the photodetector.

### 3.3 Buidling the full contrast trace

In order to build a full contrast trace, we performed a set of complete acquisitions over the same time window with varying neutral density filters: 0.5, 1, 2 and 2.5. The resulting traces are shown in figure 6. With these, it was possible to construct the global contrast trace by concatenation, as shown in figure 7. The low-level pedestal is ultimately caused by the detection limit of the diagnostic, caused by several noise sources.

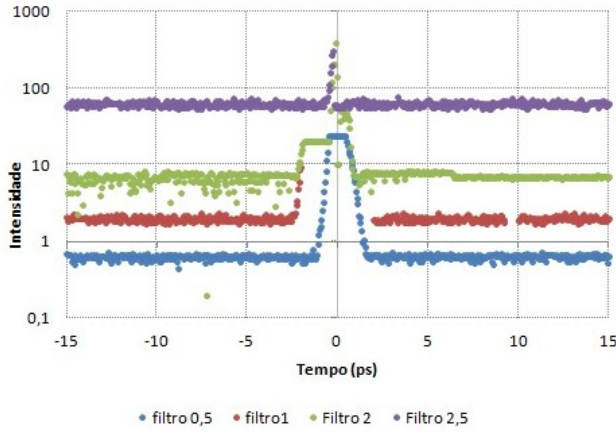


Figure 6: Data measured with a set of neutral density filters.

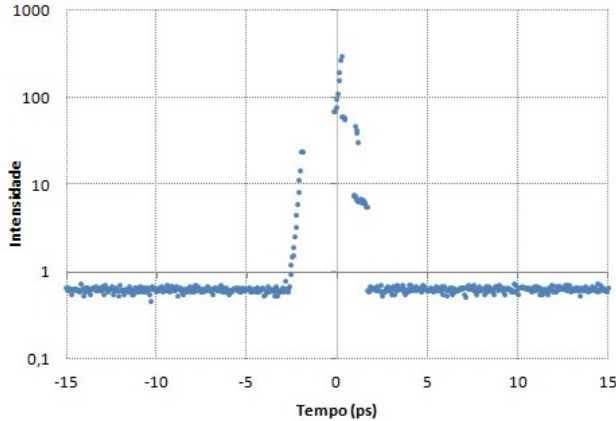


Figure 7: Concatenated contrast trace.

### 3.4 Influence of noise sources on the contrast

We also performed a preliminary study of the sources of noise in the results, i.e. the causes that ultimately limit the maximum contrast attainable. Figure5 show the

variation in the minimum trace level (in the absence of visible idler) in different experimental condition, listed on the table.

Interval (ps)	Conditions
< -17	no change
-17 to -16	pump beam blocked
-16 to -15	signal beam blocked
-15 to -14	no change
-14 to -13	no HV noise
> -13	no input

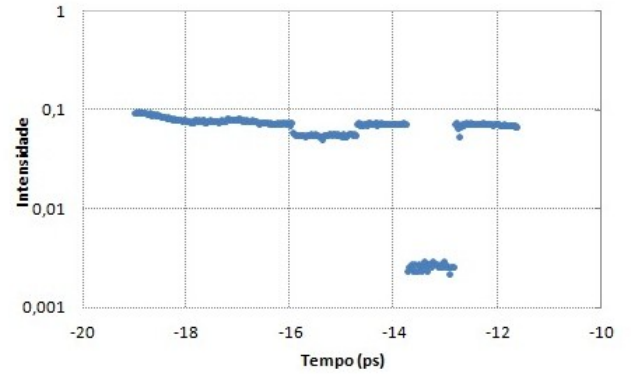


Figure 8: Influence of different noise sources.

We can conclude that one of the major sources of electronic noise is the high-voltage pulser driving the Pockels cells in the regenerative amplifier. When the acquisition setup is taken away by a meter, the noise level decreases. Other major causes of noise are scattering of the signal beam into the idler direction from the crystal, as evidenced by the level between -16 and -15 ps.

## 4 Conclusions

The OPAC was developed, implemented and its performance demonstrated successfully. The software that allows the control of the motor and the data acquisition was developed and operated. We demonstrated the ability of OPAC to work in the field and characterized the laser system at the pre-amplifier level a time window from a few to 100 ps. It was possible to make preliminary measurements of the laser contrast. Suggestions for future improvements include further automatization of the setup by controlling the voltage response of the oscilloscope, and reducing the amount of scattered signal light by using a higher optical quality OPA crystal. A detailed contrast characterization of improvement, which is outside the scope of this work, should

then be possible.

## References

- [1] G.A. Mourou, T. Tajima, S.V. Bulanov, "Optics in the relativistic regime", *Rev. Mod. Phys.* 78, 309 (2006).
- [2] V. Yanovsky, V. Chvykov, G. Kalinchenko, P. Rousseau, T. Planchon, T. Matsuoka, A. Maksimchuk, J. Nees, G. Cheriaux, G. Mourou, and K. Krushelnick, "Ultra-high intensity-300-TW laser at 0.1 Hz repetition rate", *Opt. Express* 16, 2109 (2008).
- [3] L. Antonucci, J.P. Rousseau, A. Jullien, B. Mercier, V. Laude, G. Cheriaux, "14-fs high temporal quality injector for ultra-high intensity laser", *Opt. Comm.* 282, 1374 (2009).
- [4] C. Thauray, F. Quéré, J.P. Geindre, A. Levy, T. Ceccotti, P. Monot, M. Bougeard, F. Réau, P. d'Oliveira, P. Audebert, R. Marjoribanks, P. Martin, "Plasma mirrors for ultrahigh-intensity optics", *Nat. Phys.* 3, 424 (2007).
- [5] A. Jullien, O. Albert, F. Burgy, G. Hamoniaux, J.P. Rousseau, J.P. Chambaret, F. Augé-Rochereau, G. Chériaux, J. Etchepare, N. Minkovski, S.M. Saltiel, " $10^{-10}$  temporal contrast for femtosecond ultraintense lasers by cross-polarized wave generation", *Opt. Lett.* 30, 920 (2005).
- [6] K. Sala, G. Kenney-Wallace, and G. Hall, "CW autocorrelation measurements of picosecond laser pulses", *IEEE J. Quantum Electron.* QE-16, 990 (1980).
- [7] A. Braun, D. Kopf, I. Jung, J. Rudd, H. Cheng, G. Mourou, K. Weingarten, and U. Keller, "Characterization of short-pulse oscillators by means of a high-dynamic-range autocorrelation measurement", *Opt. Lett.* 20, 1889 (1995).
- [8] S. Luan, M. H. R. Hutchinson, R. A. Smith, and F. Zhou, "High dynamic range third-order correlation measurement of picosecond laser pulse shapes", *Meas. Sci. Technol.* 4, 1426 (1993).
- [9] D. Meshulach, Y. Barad, and Y. Silberberg, "Measurement of ultrashort optical pulses by third-harmonic generation", *J. Opt. Soc. Am. B* 14, 2122 (1997).
- [10] V. Sirutkaitis, R. Grigonis, A. Piskarskas, A. Persson, and S. Svanberg, "Single-shot third-order correlator for femtosecond pulse shape investigations of terawatt power Ti:sapphire lasers", *Lith. J. Phys.* 38, 79 (1998).
- [11] J. Collier, C. Hernandez-Gomez, R. Allot, C. Danson, and A. Hill, "A single shot 3rd order auto-correlator for pulse contrast and pulse shape measurements", *Laser Part. Beams* 19, 231 (2001).
- [12] S. Montant, D. Villate, C. Rouyer, "Single shot temporal contrast measurement of subpicosecond pulses", *J. Phys.: Conf. Ser.* 244, 032011 (2010)
- [13] F. Tavella, K. Schmid, N. Ishii, A. Marcinkevičius, L. Veisz, F. Krausz, "High-dynamic range pulse-contrast measurements of a broadband optical parametric chirped-pulse amplifier", *Appl. Phys. B* 81, 753 (2005).
- [14] G. Dikchys, R. Danelius, V. Kabelka, A. Piskarskas, T. Tomkevicius, and A. Stabinis, "Parametric amplification and generation of ultrashort light pulses for spectroscopic applications", *Sov. J. Quantum Electron.* 6, 425 (1976).
- [15] A. Piskarskas, "Picosecond spectroscopy based on parametric amplification and generation of light", *Sov. J. Quantum Electron.* 6, 1019 (1976).
- [16] E. J. Divall, I. N. Ross, "High dynamic range contrast measurements by use of an optical parametric amplifier correlator", *Opt. Lett.* 29, 2273 (2005).
- [17] G. Figueira, N. Lopes, L. Cardoso, J. Wemans, J. M. Dias, M. Fajardo, C. Leitão, and J. T. Mendonça, "Performance and characterization of a 2.8 TW Ti:sapphire-Nd:glass chirped pulse amplification laser system" in *Proceedings of XV International Symposium on Gas Flow Chemical Lasers and High-Power Lasers* (J. Kody Mora, ed.) *Proc. SPIE* 5777, 636 (2005).